

Strong photon coupling to high-frequency antiferromagnetic magnons via topological surface states

Henrik T. Kaarbø,* Henning G. Hugdal,* and Sol H. Jacobsen

Center for Quantum Spintronics, Department of Physics, NTNU,
Norwegian University of Science and Technology, NO-7491 Trondheim, Norway

We show strong coupling between antiferromagnetic magnons and microwave cavity photons at both high and externally controllable magnon frequencies. Using the fully quantum mechanical path-integral method, we study an antiferromagnetic insulator (AFM) interfaced with a topological insulator (TI), taking $\text{Bi}_2\text{Se}_3\text{-MnSe}$ as a representative example. We show that the mutual coupling of the spin-polarized surface states of the TI to both the squeezed magnons and the circularly polarized cavity photons results in a Chern-Simons term that activates the stronger electric, rather than magnetic, dipole coupling. Moreover, a squeezing-mediated enhancement of the coupling is achieved due to the unequal interfacial exchange coupling to the AFM sublattices, resulting in a coupling strength up to several orders stronger than for direct magnon-photon coupling. While direct cavity-AFM coupling has so far been limited in its applicability due to weak or low frequency coupling, this result may advance the utilization of high-frequency cavity magnonics and enable its incorporation into quantum information technology.

Strong coupling between magnons and microwave photons in cavities [1–7] opens numerous possibilities for probing magnonic states [8, 9], inducing unconventional spin states [10], and bridging spintronics and optics-based quantum information technology [11–14]. The Zeeman coupling between isolated spins and cavity photons is in itself not strong, with a coupling constant of the order of the Bohr magneton. Magnons, being collective excitations of N spins, attain an additional scaling factor \sqrt{N} . Taken together with the confinement of electromagnetic waves in cavity systems, this gives rise to strong coupling in systems with a macroscopic number of spins, such as ferromagnetic (FM) insulators. In principle, antiferromagnetic (AFM) insulators can also be strongly coupled to photons, but the reduced magnetic moment due to opposite spin alignment significantly reduces the coupling strength [13]. Strong coupling to AFMs has therefore only been shown for quasi-AFM phases with a finite magnetic moment [4, 15], or at low frequencies [7].

The ratio of the magnetic and electric dipole coupling is proportional to the fine structure constant [13], and achieving an electric coupling between photons and magnons could therefore lead to an increased coupling. However, the bound charges in FMs and AFMs do not couple resonantly to the electric cavity field to leading order. It is therefore generally overlooked as a coupling mechanism in cavities without driving, but has recently been shown to be relevant for photonic coupling to spin-flip excitations in metallic multi-band ferromagnets, where the magnons couple exclusively to either left- or right-handed circularly polarized cavity photons [16]. Moreover, Lee *et al* [17] recently proposed that the electric-field coupling can be boosted by an effective photon-magnon coupling achieved via a Chern-Simons (CS) term [18–21] that appears when the spin-polarized surface states of a topological insulator (TI) mutually couple to both FM-magnons and cavity photons. A CS term also appears in the effective theory of AFM magnons coupled to a TI, as long as there is a finite mass gap in the TI surface state dispersion [19, 21], which can be achieved via magnetic doping at the interface [22–27] or an uncompensated AFM interface [27–30] [see Fig. 1(b)]. Since

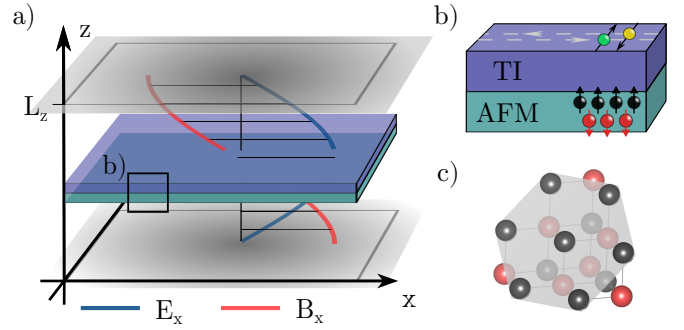


FIG. 1. (a) A bilayer comprising a thin AFM and TI is placed at the electric field maxima of an electromagnetic cavity. (b) The TI is interfaced to an uncompensated edge of the AFM, which hosts spins from the sublattice pointing perpendicularly out of (black) or into (red) the interfacing plane, generating squeezed magnonic modes. The spin-polarized surface states on the TI (green/yellow) couple to both the AFM squeezed magnons and cavity photons. (c) Structure of the interfacial (111)-plane of the AFM bipartite sublattices.

easy-axis AFMs host magnons with two polarization axes [31], they therefore allow for selective coupling to the circularly-polarized cavity photons, which we will show can be tuned and greatly boosted via interactions with a TI.

Similarly to FM magnons, AFM magnons have unit spin. However, the AFM magnon eigenstates do not correspond to spin flips in one of the sublattices, denoted sublattice magnons, but are rather superpositions of large numbers of sublattice magnons with total spin equal to \hbar . The eigenstates are *two-mode squeezed magnons* [32, 33]. Therefore, a particle with different interaction strengths to the spins of the two AFM sublattices, for example via an uncompensated interface, can have an enhanced coupling to AFM magnons due to the dramatic increase in the effective magnon spin coupling to the particle – a process termed *squeezing-mediated coupling enhancement* [32], measurable via qubit excitation spectroscopy [34, 35], for example. This has been shown to increase the superconducting and exciton magnon-mediated pairing [36–40], and has been proposed as a possible mechanism for increasing

magnon-photon coupling in ferrimagnets [41] and easy-axis FMs [42].

In this letter, we use the quantum path integral method to show that a TI-AFM bilayer in an electromagnetic cavity can be employed to harness the potential of strong electric dipolar coupling (see Fig. 1). The spin-polarized surface states of the TI couple jointly to the cavity photons and the squeezed magnons, with a large squeezing-mediated coupling enhancement when the interface is uncompensated. This leads to a dramatic enhancement in the effective magnon-photon coupling, with coupling strengths far exceeding those previously achieved in cavity systems. As the coupling is proportional to the AFM magnon frequency, this approach naturally allows for strong coupling at high frequencies.

The cavity-bilayer system of Fig. 1 is described by the action $S = S_{\text{cav}}^0 + S_{\text{mag}}^0 + S_{\text{TI}}$, where the interactions are included in S_{TI} , and the bare cavity and magnon terms are ($\hbar = 1$)

$$S_{\text{cav}}^0 = - \sum_q \sum_{l=L,R} a_{ql}^\dagger (i\Omega_n - \omega_{\mathbf{q}}) a_{ql}, \quad (1)$$

$$S_{\text{mag}}^0 = - \sum_q \sum_{l=L,R} \mu_{ql}^\dagger (i\Omega_n - \omega_{\mathbf{q}}) \mu_{ql}. \quad (2)$$

The bosonic fields $a_{ql}^{(\dagger)}$ describe left- (L) and right-handed (R) circularly polarized photons, and $\mu_{ql}^{(\dagger)}$ describe the two branches of antiferromagnetic squeezed magnons in a bipartite lattice [32], which in easy-axis AFMs are L- and R-handed circularly polarized [31]. Since the R (L) photons and magnons both have spin $+\hbar$ ($-\hbar$) [43, 44], the parameter l will be used to denote the polarization ($l = R/L$) and the spin quantum number ($l = \pm 1$). The three-vector $q = (\Omega_n, \mathbf{q})$, with momentum \mathbf{q} in the xy plane and bosonic Matsubara frequency $\Omega_n = 2\pi n/\beta$, for $n \in \mathbb{Z}$ and $\beta = 1/k_{\text{B}}T$, where k_{B} is the Boltzmann constant and T the system temperature [18]. Assuming that the in-plane cavity dimensions are much larger than the height L_z , we focus on modes with $n_z = 1$, such that the cavity mode dispersion is $\omega_{\mathbf{q}} = c\sqrt{\pi^2/L_z^2 + \mathbf{q}^2}$, with speed of light c . For an AFM with easy-axis anisotropy in a static magnetic field along z , the magnon branches are given by [45, 46]

$$\omega_{\mathbf{q}l} = \sqrt{(1 - \gamma_{\mathbf{q}}^2)\omega_E^2 + \omega_K(2\omega_E + \omega_K) + l\omega_H}. \quad (3)$$

Here, ω_E, ω_K and ω_H are the characteristic frequencies of the exchange interaction, easy-axis anisotropy and magnetic field, respectively, and $\gamma_{\mathbf{q}} = N_\delta^{-1} \sum_{\{\delta\}} e^{i\mathbf{q}\cdot\delta}$, where $\{\delta\}$ is the set of N_δ nearest neighbor lattice vectors [47].

The TI action in imaginary time (τ) and position (\mathbf{r}) space, including interactions with the cavity and AFM is [21, 48]

$$S_{\text{TI}} = \int_0^\beta d\tau \int d\mathbf{r} \psi^\dagger \left[\partial_\tau - (iv_{\text{F}} \nabla + \tilde{\mathbf{A}}) \cdot \boldsymbol{\sigma} - m\sigma_z \right] \psi, \quad (4)$$

where $\psi = (\psi_\uparrow \psi_\downarrow)^T$ with spin-up and -down fermion fields, $\boldsymbol{\sigma} = (\sigma_y, -\sigma_x)$ is the rotated 2D Pauli vector, and v_{F} is the TI's Fermi velocity. Note that terms without explicit matrix

structure are implicitly taken to be proportional to the identity matrix throughout. We have also defined the effective vector potential

$$\tilde{\mathbf{A}} = v_{\text{F}} e \mathbf{A} + (J_A \mathbf{S}_A^\parallel + J_B \mathbf{S}_B^\parallel) \times \hat{z}, \quad (5)$$

where e is the electron charge, \hat{z} is the unit vector along z , and the TI mass gap $m = J_A S_A^z + J_B S_B^z$. The in-plane cavity vector potential is \mathbf{A} , and \mathbf{S}_s^\parallel and S_s^z are the in-plane and out-of-plane components of the AFM spin distribution on sublattice $s = A, B$ with coupling constant J_s . Assuming that the spins on the two sublattices have magnitude S and are ordered in the $+\hat{z}$ and $-\hat{z}$ directions, we get $m = S(J_A - J_B)$ and can treat the in-plane spin terms as fluctuations. The average cavity vector potential is also small for an undriven cavity, and the contributions from $\tilde{\mathbf{A}}$ can be treated as small compared to the remaining terms in the TI action, collected in the inverse Green's function $G^{-1} = -\partial_\tau + iv_{\text{F}} \nabla \cdot \boldsymbol{\sigma} + m\sigma_z$. The direct interaction between the cavity and AFM is neglected, since it is weak compared to the effective interaction induced by the TI surface states.

Performing the Gaussian integral over fermionic fields results in a term $-\text{Tr} \ln(-G^{-1} + \tilde{\mathbf{A}} \cdot \boldsymbol{\sigma})$ in the system action, which to leading order in $G|\tilde{\mathbf{A}}|$ leads to an additional term in the combined photon and magnon action, $S_{\text{cav}} + S_{\text{mag}} = S_{\text{cav}}^0 + S_{\text{mag}}^0 + \delta S$ [18, 21], where

$$\delta S = \frac{1}{2} \sum_{kq} \text{tr} G_k \tilde{\mathbf{A}}_q \cdot \boldsymbol{\sigma} G_{k-q} \tilde{\mathbf{A}}_{-q} \cdot \boldsymbol{\sigma}. \quad (6)$$

The above is written using three-vector k and spin basis of the TI surface states, where $k = (\omega_n, \mathbf{k})$ with fermion Matsubara frequency ω_n and momentum \mathbf{k} . In this basis, the TI Green's function is

$$G_k = \frac{i\omega_n + v_{\text{F}} \mathbf{k} \cdot \boldsymbol{\sigma} - m\sigma_z}{(i\omega_n - \epsilon_{\mathbf{k}})(i\omega_n + \epsilon_{\mathbf{k}})}, \quad (7)$$

with surface state dispersion relation $\epsilon_{\mathbf{k}} = \sqrt{(v_{\text{F}} \mathbf{k})^2 + m^2}$. Performing the trace over spin states and the sum over k in Eq. (6) leads to a topological CS term

$$S_{\text{CS}} = \sum_q \frac{A\beta m}{8\pi v_{\text{F}}^2 |m|} \Omega_n (\tilde{\mathbf{A}}_q \times \tilde{\mathbf{A}}_{-q}) \cdot \hat{z}, \quad (8)$$

where A is the TI-AFM interface area. We neglect the Maxwell and anisotropy terms that also appear [21], since they either only renormalize the photon and magnon theories, or lead to magnon-photon coupling terms that are weaker than the CS term. The effective vector potential [Eq. (5)] in Matsubara and Fourier-space is

$$\begin{aligned} \tilde{\mathbf{A}}_q = & \frac{iv_{\text{F}} e}{\sqrt{\epsilon_0 \omega_{\mathbf{q}} V \beta}} \sum_l \mathbf{e}_l e^{il\phi_{\mathbf{q}}} (a_{ql} + a_{-q\bar{l}}^\dagger) \\ & + i \sqrt{\frac{S}{N\beta}} \left[\mathbf{e}_L (J_A m_{-qA}^\dagger + J_B m_{qB}) \right. \\ & \left. - \mathbf{e}_R (J_A m_{qA} + J_B m_{-qB}^\dagger) \right], \end{aligned} \quad (9)$$

where we have written the cavity vector potential in terms of the photon fields [49, 50] and performed the Holstein-Primakoff transformation for the spins [51]. Here, $V = AL_z$ is the cavity volume, $m_{qA(B)}$ are the magnon fields for the A(B) sublattice, and we have defined the polarization vectors $\mathbf{e}_{L/R} = (\hat{x} \pm i\hat{y})/\sqrt{2}$. The angle of \mathbf{q} relative to the q_x axis is $\phi_{\mathbf{q}}$, and \bar{l} denotes the opposite polarization of l . Since $\hat{\mathbf{A}}$ contains both cavity and magnon fields, Eq. (8) leads to corrections to both the cavity and spin theories through a (small) renormalization of their respective Matsubara frequencies and thus their dispersion (which we hereafter assume to be included in $\omega_{\mathbf{q}}$). Their cross terms, however, leave an effective coupling between the cavity and AFM spins, which we will further elucidate.

The AFM action is not diagonal in the sublattice magnon fields $m_{qA/B}$, but rather for the squeezed magnons, related by the Bogoliubov transformation [32, 46]

$$\mu_{qR} = u_{\mathbf{q}}m_{qA} + v_{\mathbf{q}}m_{-qB}^\dagger, \quad (10a)$$

$$\mu_{qL} = u_{\mathbf{q}}m_{qB} + v_{\mathbf{q}}m_{-qA}^\dagger, \quad (10b)$$

where $u_{\mathbf{q}}(v_{\mathbf{q}}) = \sqrt{\frac{\omega_E + \omega_K}{\omega_{\mathbf{q}R} + \omega_{\mathbf{q}L}} \pm \frac{1}{2}}$. To find the magnon-photon coupling, we therefore insert Eqs. (9) and (10) into Eq. (8). Keeping only terms with both photon and magnon fields, we get the interaction

$$S_{\text{int}} = \sum_q i\Omega_n \kappa_{\mathbf{q}} \left[\begin{pmatrix} \mu_{qR}^\dagger & \mu_{-qL} \end{pmatrix} V_{\mathbf{q}} \begin{pmatrix} a_{qR} \\ a_{-qL}^\dagger \end{pmatrix} + \begin{pmatrix} a_{qR}^\dagger & a_{-qL} \end{pmatrix} V_{\mathbf{q}}^\dagger \begin{pmatrix} \mu_{qR} \\ \mu_{-qL}^\dagger \end{pmatrix} \right], \quad (11)$$

with dimensionless interaction matrix

$$V_{\mathbf{q}} = [(u_{\mathbf{q}} - v_{\mathbf{q}})(\sigma_0 + \sigma_x) + \Delta(u_{\mathbf{q}} + v_{\mathbf{q}})(\sigma_z + i\sigma_y)]e^{i\phi_{\mathbf{q}}}, \quad (12)$$

and function $\kappa_{\mathbf{q}} = -\frac{JAm_e}{4\pi v_F |m|} \sqrt{\frac{S}{\epsilon_0 \omega_{\mathbf{q}} NV}}$, where $J = (J_A + J_B)/2$ and $\Delta = (J_A - J_B)/(J_A + J_B)$.

The interaction in Eqs. (11) and (12) displays two important properties and benefits of an AFM compared to a FM: (1) The coupling is proportional to the frequency $i\Omega_n \rightarrow \omega_{\mathbf{q}l}$, which is orders of magnitude higher for AFMs; (2) If the coupling of the TI to the two sublattices is unequal ($\Delta \neq 0$), the interaction strength can be increased dramatically. In the long wavelength limit, we have $u_{\mathbf{q}} \pm v_{\mathbf{q}} \sim (2\omega_E/\omega_K)^{\pm 1/4}$, which means that for ratios $\omega_E/\omega_K \sim 10^4$ [32] it is possible to increase the effective magnon-photon coupling by up to two orders of magnitude due to squeezing-enhancement when $\Delta \neq 0$, compared to coupling equally to the sublattice magnons ($\Delta = 0$).

The effect of the increase in magnon-photon coupling due to these two mechanisms can be illustrated by considering changes to the photon resonances in Fig. 2. Integrating out the magnon modes [18], we get the effective cavity theory,

$$S_{\text{cav}} = - \sum_q \begin{pmatrix} a_{qR}^\dagger & a_{-qL} \end{pmatrix} D_q^{-1} \begin{pmatrix} a_{qR} \\ a_{-qL}^\dagger \end{pmatrix}. \quad (13)$$

Here, the inverse Green's function

$$D_q^{-1} = \begin{pmatrix} i\Omega_n - \omega_{\mathbf{q}} - \Pi_q & -\Pi_q \\ -\Pi_q & -i\Omega_n - \omega_{\mathbf{q}} - \Pi_q \end{pmatrix}, \quad (14)$$

whose self-energy due to coupling to magnons is given by

$$\Pi_q = -\Omega_n^2 \left\{ \frac{g_{\mathbf{q}R}^2}{i\Omega_n - \omega_{\mathbf{q}R}} - \frac{g_{\mathbf{q}L}^2}{i\Omega_n + \omega_{\mathbf{q}L}} \right\}, \quad (15)$$

where

$$g_{\mathbf{q}l} = |\kappa_{\mathbf{q}}| |u_{\mathbf{q}} - v_{\mathbf{q}} + l\Delta(u_{\mathbf{q}} + v_{\mathbf{q}})|. \quad (16)$$

Inverting Eq. (14), we find the Green's functions for the R- and L- photons [16]

$$D_{ql} = \frac{i\Omega_n + \omega_{\mathbf{q}} + \Pi_{lq}}{(i\Omega_n)^2 - \omega_{\mathbf{q}}^2 - 2\omega_{\mathbf{q}}\Pi_{lq}}, \quad (17)$$

where the self-energy is evaluated at momenta $lq = \pm q$ for R/L modes.

The photon dispersion in the interacting system are found by analytically continuing to real frequencies, $i\Omega_n \rightarrow \Omega + i\delta$, where $\delta = 0^+$, and finding the zeros of the denominator in Eq. (17). The resulting root equation is fourth order in Ω , but can be reduced to a cubic equation by disregarding negative energy solutions, i.e., letting $\Omega + \omega_{\mathbf{q}} \rightarrow 2\omega_{\mathbf{q}}$. Moreover, only one of the two terms in Eq. (15) contribute significantly depending on the sign of q in Eq. (17). Neglecting the far off-resonant term, we get two solutions corresponding to the magnon-polariton modes for each polarization,

$$\omega_{l\pm} = \frac{\omega_{\mathbf{q}} + \omega_{\mathbf{q}l}}{2(1 - g_{\mathbf{q}l}^2)} \pm \frac{\sqrt{(\omega_{\mathbf{q}} - \omega_{\mathbf{q}l})^2 + 4\omega_{\mathbf{q}}\omega_{\mathbf{q}l}g_{\mathbf{q}l}^2}}{2(1 - g_{\mathbf{q}l}^2)}. \quad (18)$$

For $|\omega_{\mathbf{q}} - \omega_{\mathbf{q}l}| \gg 2g_{\mathbf{q}l}\sqrt{\omega_{\mathbf{q}}\omega_{\mathbf{q}l}}$ and $\omega_{\mathbf{q}} > \omega_{\mathbf{q}l}$ ($\omega_{\mathbf{q}} < \omega_{\mathbf{q}l}$), the solution with upper (lower) sign approaches $\omega_{\mathbf{q}}$, while the lower (upper) sign solution approaches $\omega_{\mathbf{q}l}$. For $\omega_{\mathbf{q}} = \omega_{\mathbf{q}l}$, the frequency splitting between the resonances is $2\omega_{\mathbf{q}}g_{\mathbf{q}l} \equiv 2\tilde{g}_{\mathbf{q}l}$ meaning that the effective coupling strength between magnons and photons with polarization l is approximately

$$\tilde{g}_{\mathbf{q}l} \approx \frac{em(u_{\mathbf{q}} + v_{\mathbf{q}})}{8\pi v_F} \sqrt{\frac{\omega_{\mathbf{q}} A_{\text{uc}}}{\epsilon_0 S L_z}} \approx \frac{em}{4\pi v_F} \sqrt{\frac{\omega_E A_{\text{uc}}}{2\epsilon_0 S L_z}}, \quad (19)$$

where AFM unit cell area $A_{\text{uc}} = A/N$. In the case of no sublattice compensation, $\Delta = 1$, substituting $(u_{\mathbf{q}} + v_{\mathbf{q}}) \rightarrow 2u_{\mathbf{q}}(2v_{\mathbf{q}})$ in Eq. (19) gives $g_{\mathbf{q}R}(g_{\mathbf{q}L})$. In the limit $\mathbf{q} \rightarrow 0$ and $\omega_K, \omega_H \ll \omega_E$, this difference is negligible, giving the last approximation, which elucidates the advantage of using an uncompensated AFM versus a regular ferromagnet. At resonance, the coupling strength effectively depends on the characteristic exchange frequency ω_E , which is typically an order of magnitude larger than the uniform mode frequencies for AFMs, and several orders of magnitude larger than its FM counterpart. This coupling is most readily compared to the

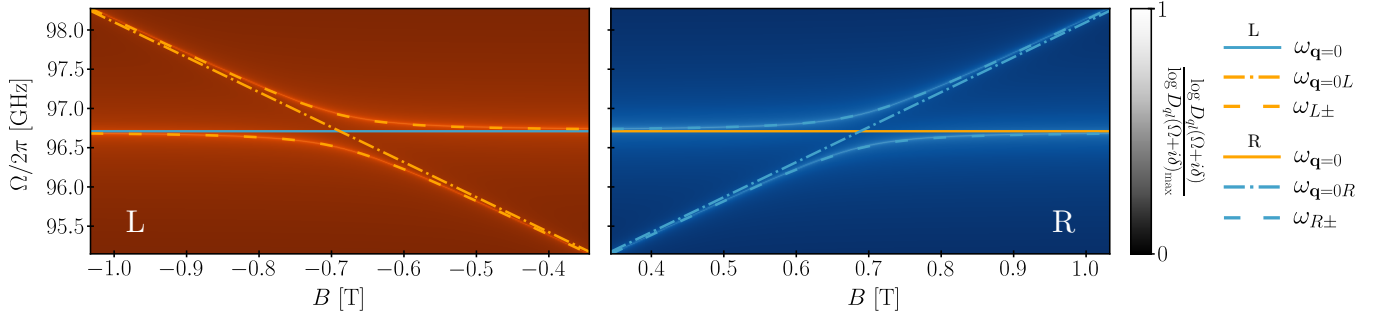


FIG. 2. Colorplots of the L- and R- photons' spectral functions [Eq. (17)] for different applied magnetic fields, with small but finite imaginary component $\delta = 10^{-15}$ rad/sec and approximate solutions for $\omega_{L\pm}$ [Eq. (18)], showing strong coupling via an avoided crossing with an approximate gap of 0.5 GHz at magnon-photon resonance. System parameters are presented in the main text.

magnon-photon coupling g_{qZ} based on the Zeeman interaction in antiferromagnets, given by [45]

$$g_{qZ} = \frac{|\gamma|}{c} \sqrt{\frac{\omega_{\mathbf{q}} S}{\epsilon_0 A_{uc} L_z}} (u_{\mathbf{q}} - v_{\mathbf{q}}), \quad (20)$$

where γ is the gyromagnetic ratio. The relative coupling enhancement $\Gamma_{\mathbf{q}} = \tilde{g}_{\mathbf{q}}/g_{qZ}$ is thus given by

$$\Gamma_{\mathbf{q}} = \frac{emcA_{uc}}{8\pi v_F S |\gamma|} \frac{(u_{\mathbf{q}} + v_{\mathbf{q}})}{(u_{\mathbf{q}} - v_{\mathbf{q}})} \approx \frac{emcA_{uc}}{8\pi v_F S |\gamma|} \sqrt{\frac{2\omega_E}{\omega_K}}. \quad (21)$$

To estimate the coupling strength, we consider the specific TI-AFM bilayer of Bi_2Se_3 -MnSe, which is an experimentally well-studied heterostructure [28, 29, 52, 53]. An alternative could be Bi_2Se_3 -CrI₃ [54], where bilayer CrI₃ is shown to have antiferromagnetically coupled FM layers [55–57]. For the TI we use $v_F = 3 \times 10^5$ m/s [29, 58], and for the AFM we set the spin $S = 2.5$ [59], $A_{uc} = 0.13$ nm² [52], and $\omega_E/\omega_K \sim 10^3$ to 10^4 [32, 60]. For the induced mass gap we use $m = 45$ meV [28, 52]. Using these parameters, the relative enhancement of the magnon-photon interaction is $\Gamma_{q=0} \sim 50$ to 170, i.e. showing that the coupling strength is comfortably enhanced by up to two orders.

In Fig. 2, we show avoided crossings in the L/R-polarized photon dispersion curves as the characteristic signature of their strong coupling to the different magnon branches. We set $L_z = 1.55$ nm for the $n_z = 1$ cavity mode to be close to the relevant uniform mode frequency of the AFM with exchange parameter $|J_{AB}| = 1$ meV, whose value does not affect the coupling enhancement when ω_E/ω_K remains constant. The dependence of the uniform magnon modes' frequencies on the static external magnetic field makes it possible to select for photons of a specific chirality. A modulation of the external field could then switch an unpolarized photon signal from being transmitted to one magnon branch and then the other, acting as a signal splitter, or frequency-dependent linear-to-circular polarization converter [61], and providing a mechanism for non-invasive cavity engineering [16, 62].

The analytic expressions [Eq. (18)] and numerical results [using Eq. (17)] shown in Fig. 2 are in excellent agreement.

The numerical results do not explicitly include the correction to the magnon dispersion due to interaction with the TI, e.g. from the magnon-magnon terms in Eq. (8), which would in practice result in a small, degeneracy lifting renormalization of the magnon branches [21]. However, a notable consequence of the renormalization is that the magnons take on an anyonic character [18] in the two-dimensional limit by breaking the $2\pi n/\beta$ -periodicity of the magnonic Matsubara frequencies Ω_n .

We emphasize that the strong coupling enhancement predicted here is an interface effect, which cannot be further enhanced by adding magnetic layers in the bulk (increasing N) as is often employed for maximizing magnetic dipole coupling. However, as $g_{qZ} \sim \sqrt{N/V} \sim 1/\sqrt{A_{uc} L_z}$, the coupling increase is not due to the increased numbers of spin directly, but rather the increase in geometrical overlap factor when increasing the magnetic volume. Still we expect the coupling predicted herein to rival the standard Zeeman effect, and emphasize that the overlap factor can be increased by cavity engineering, relevant for both coupling mechanisms, in addition to increasing the magnet volume [6]. Unlike bulk Zeeman-based coupling, which requires that the photon and excited magnon's wavelengths correspond across the bulk to generate coherent excitations [63], the bilayer acts as a strong photomagnonic spin pump at the AFM/TI interface. This is advantageous, as the generated magnon only needs to be in-phase with the photon at the interface, before propagating into a neighboring magnetic material, in analogy to heavy-metal induced spin-orbit torque [63]. The coupling mechanism introduced here may therefore enable photonic control of coherent excitations in ultrafast antiferromagnetic spintronics devices.

Strong coupling shows that magnonic and photonic information can be mutually exchanged and manipulated in microwave cavities. Its potential could be further developed by exploiting the external control for signal splitting, for example via a quasi-static oscillating field, and exploring the extent to which this mechanism may also be used to control other time-reversal symmetry-breaking systems which couple to only one of the photon modes. In addition, one can investigate the consequences for strong coupling to qubits [35], or to superconducting reservoirs, which also couple via the electric field [50, 64].

Other materials with strong spin-orbit coupling, and coupling via other spin Hall effects [65, 66], may provide interesting alternatives to the TI. Furthermore, metallic AFMs can have much higher Néel temperatures, and could therefore also offer very strong coupling in bilayer setups like the one proposed. Moreover, since charge-transport can reposition the Néel vector between the gapped and gapless phases in topological metallic AFMs [67], their use in a similar setup could provide an externally tunable way to manipulate the AFM-ordering, and provide a potential mechanism for dual read-write protocols.

We have shown strong, tunable, high-frequency coupling between AFM magnons and circularly polarized microwave cavity photons. This is mediated by a Chern-Simons term that appears due to the mutual coupling of the spin-polarized surface states of a TI to both the squeezed magnons and the cavity photons. This activates the strong electric dipole coupling, which is seen here to be up to several orders stronger than direct magnon-photon coupling for a representative $\text{Bi}_2\text{Se}_3\text{-MnSe}$ example. Experimental confirmation of this prediction would be a significant step towards the ambition of incorporating high-frequency magnonics with photonic quantum information technologies.

Acknowledgments. We acknowledge funding via the “Outstanding Academic Fellows” programme at NTNU and the Research Council of Norway Grant Nos. 302315 and 262633.

* These two authors contributed equally

- [1] Hans Huebl, Christoph W. Zollitsch, Johannes Lotze, Fredrik Hocke, Moritz Greifenstein, Achim Marx, Rudolf Gross, and Sebastian T.B. Goennenwein, “High cooperativity in coupled microwave resonator ferrimagnetic insulator hybrids,” *Physical Review Letters* **111**, 127003 (2013).
- [2] Yutaka Tabuchi, Seiichiro Ishino, Toyofumi Ishikawa, Rekishu Yamazaki, Koji Usami, and Yasunobu Nakamura, “Hybridizing ferromagnetic magnons and microwave photons in the quantum limit,” *Physical Review Letters* **113**, 083603 (2014).
- [3] Xufeng Zhang, Chang-Ling Zou, Liang Jiang, and Hong X. Tang, “Strongly Coupled Magnons and Cavity Microwave Photons,” *Physical Review Letters* **113**, 156401 (2014).
- [4] M. Białek, J. Zhang, H. Yu, and J.-Ph. Ansermet, “Strong Coupling of Antiferromagnetic Resonance with Subterahertz Cavity Fields,” *Physical Review Applied* **15**, 044018 (2021).
- [5] Matthias Mergenthaler, Junjie Liu, Jennifer J. Le Roy, Natalia Ares, Amber L. Thompson, Lapo Bogani, Fernando Luis, Stephen J. Blundell, Tom Lancaster, Arzhang Ardavan, G. Andrew D. Briggs, Peter J. Leek, and Edward A. Laird, “Strong Coupling of Microwave Photons to Antiferromagnetic Fluctuations in an Organic Magnet,” *Physical Review Letters* **119**, 147701 (2017).
- [6] Graeme Flower, Maxim Goryachev, Jeremy Bourhill, and Michael E Tobar, “Experimental implementations of cavity-magnon systems: From ultra strong coupling to applications in precision measurement,” *New Journal of Physics* **21**, 095004 (2019).
- [7] I. Boventer, H. T. Simensen, B. Brekke, M. Weides, A. Anane, M. Kläui, A. Brataas, and R. Lebrun, “Antiferromagnetic Cavity Magnon Polaritons in Collinear and Canted Phases of Hematite,” *Physical Review Applied* **19**, 014071 (2023).
- [8] Dany Lachance-Quirion, Yutaka Tabuchi, Seiichiro Ishino, Atsushi Noguchi, Toyofumi Ishikawa, Rekishu Yamazaki, and Yasunobu Nakamura, “Resolving quanta of collective spin excitations in a millimeter-sized ferromagnet,” *Science Advances* **3**, e1603150 (2017).
- [9] Dany Lachance-Quirion, Samuel Piotr Wolski, Yutaka Tabuchi, Shingo Kono, Koji Usami, and Yasunobu Nakamura, “Entanglement-based single-shot detection of a single magnon with a superconducting qubit,” *Science* **367**, 425–428 (2020).
- [10] Alessio Chiochetta, Dominik Kiese, Carl Philipp Zelle, Francesco Piazza, and Sebastian Diehl, “Cavity-induced quantum spin liquids,” *Nature Communications* **12**, 5901 (2021).
- [11] Yutaka Tabuchi, Seiichiro Ishino, Atsushi Noguchi, Toyofumi Ishikawa, Rekishu Yamazaki, Koji Usami, and Yasunobu Nakamura, “Coherent coupling between a ferromagnetic magnon and a superconducting qubit,” *Science* **349**, 405–408 (2015).
- [12] Dany Lachance-Quirion, Yutaka Tabuchi, Arnaud Gloppe, Koji Usami, and Yasunobu Nakamura, “Hybrid quantum systems based on magnonics,” *Applied Physics Express* **12**, 070101 (2019).
- [13] Babak Zare Rameshti, Silvia Viola Kusminskiy, James A. Haigh, Koji Usami, Dany Lachance-Quirion, Yasunobu Nakamura, Can-Ming Hu, Hong X. Tang, Gerrit E.W. Bauer, and Yaroslav M. Blanter, “Cavity magnonics,” *Physics Reports* **979**, 1–61 (2022).
- [14] Frank Schlawin, D. M. Kennes, and M. A. Sentef, “Cavity quantum materials,” *Applied Physics Reviews* **9**, 011312 (2022).
- [15] Kirill Grishunin, Thomas Huisman, Guanqiao Li, Elena Mishina, Theo Rasing, Alexey V. Kimel, Kailing Zhang, Zuanming Jin, Shixun Cao, Wei Ren, Guo-Hong Ma, and Rostislav V. Mikhaylovskiy, “Terahertz Magnon-Polaritons in TmFeO_3 ,” *ACS Photonics* **5**, 1375–1380 (2018).
- [16] Henning G. Hugdal, Eirik Jaccheri Høydalsvik, and Sol H. Jacobsen, “Dichroic cavity mode splitting and lifetimes from interactions with a ferromagnetic metal,” *Physical Review B* **110**, L161102 (2024).
- [17] Jongjun M. Lee, Myung-Joong Hwang, and Hyun-Woo Lee, “Topological magnon-photon interaction for cavity magnonics,” *Communications Physics* **6**, 194 (2023).
- [18] Alexander Altland and Ben Simons, *Condensed Matter Field Theory*, 3rd ed. (Cambridge University Press, Cambridge, 2023).
- [19] Flavio S. Nogueira and Ilya Eremin, “Semimetal-insulator transition on the surface of a topological insulator with in-plane magnetization,” *Physical Review B* **88**, 085126 (2013).
- [20] Stefan Rex, Flavio S. Nogueira, and Asle Sudbø, “Nonlocal topological magnetoelectric effect by Coulomb interaction at a topological insulator-ferromagnet interface,” *Physical Review B* **93**, 014404 (2016).
- [21] Stefan Rex, Flavio S. Nogueira, and Asle Sudbø, “Topological staggered field electric effect with bipartite magnets,” *Physical Review B* **95**, 155430 (2017).
- [22] Qin Liu, Chao-Xing Liu, Cenke Xu, Xiao-Liang Qi, and Shou-Cheng Zhang, “Magnetic impurities on the surface of a topological insulator,” *Physical Review Letters* **102**, 156603 (2009).
- [23] Y. L. Chen, J.-H. Chu, J. G. Analytis, Z. K. Liu, K. Igarashi, H.-H. Kuo, X. L. Qi, S. K. Mo, R. G. Moore, D. H. Lu, M. Hashimoto, T. Sasagawa, S. C. Zhang, I. R. Fisher, Z. Hussain, and Z. X. Shen, “Massive dirac fermion on the surface of a magnetically doped topological insulator,” *Science* **329**, 659–662 (2010).
- [24] Su Yang Xu, Madhab Neupane, Chang Liu, Duming Zhang, Anthony Richardella, L. Andrew Wray, Nasser Alidoust, Mats Leandersson, Thiagarajan Balasubramanian, Jaime Sánchez-Barriga, Oliver Rader, Gabriel Landolt, Bartosz Slomski, Jan

- Hugo Dil, Jürg Osterwalder, Tay Rong Chang, Horng Tay Jeng, Hsin Lin, Arun Bansil, Nitin Samarth, and M. Zahid Hasan, “Hedgehog spin texture and Berry’s phase tuning in a magnetic topological insulator,” *Nature Physics* **8**, 616–622 (2012).
- [25] Minhao Liu, Jinsong Zhang, Cui-Zu Chang, Zuo Cheng Zhang, Xiao Feng, Kang Li, Ke He, Li-li Wang, Xi Chen, Xi Dai, Zhong Fang, Qi-Kun Xue, Xucun Ma, and Yayu Wang, “Crossover between Weak Antilocalization and Weak Localization in a Magnetically Doped Topological Insulator,” *Physical Review Letters* **108**, 036805 (2012).
- [26] Qing Lin He, Xufeng Kou, Alexander J. Grutter, Gen Yin, Lei Pan, Xiaoyu Che, Yuxiang Liu, Tianxiao Nie, Bin Zhang, Steven M. Disseler, Brian J. Kirby, William Ratcliff II, Qiming Shao, Koichi Murata, Xiaodan Zhu, Guoqiang Yu, Yabin Fan, Mohammad Montazeri, Xiaodong Han, Julie A. Borchers, and Kang L. Wang, “Tailoring exchange couplings in magnetic topological-insulator/antiferromagnet heterostructures,” *Nature Materials* **16**, 94–100 (2017).
- [27] Semonti Bhattacharyya, Golrokh Akhgar, Matthew Gebert, Julie Karel, Mark T. Edmonds, and Michael S. Fuhrer, “Recent Progress in Proximity Coupling of Magnetism to Topological Insulators,” *Advanced Materials* **33**, 2007795 (2021).
- [28] S. V. Eremeev, V. N. Men’shov, V. V. Tugushev, P. M. Echenique, and E. V. Chulkov, “Magnetic proximity effect at the three-dimensional topological insulator/magnetic insulator interface,” *Physical Review B* **88**, 144430 (2013).
- [29] Weidong Luo and Xiao-Liang Qi, “Massive Dirac surface states in topological insulator/magnetic insulator heterostructures,” *Physical Review B* **87**, 085431 (2013).
- [30] Sergey V. Eremeev, Mikhail M. Otrokov, and Evgueni V. Chulkov, “New Universal Type of Interface in the Magnetic Insulator/Topological Insulator Heterostructures,” *Nano Letters* **18**, 6521–6529 (2018).
- [31] Jiahao Han, Ran Cheng, Luqiao Liu, Hideo Ohno, and Shunsuke Fukami, “Coherent antiferromagnetic spintronics,” *Nature Materials* (2023), 10.1038/s41563-023-01492-6.
- [32] Akashdeep Kamra, Even Thingstad, Gianluca Rastelli, Rembert A. Duine, Arne Brataas, Wolfgang Belzig, and Asle Sudbø, “Antiferromagnetic magnons as highly squeezed Fock states underlying quantum correlations,” *Physical Review B* **100**, 174407 (2019).
- [33] Akashdeep Kamra, Wolfgang Belzig, and Arne Brataas, “Magnon-squeezing as a niche of quantum magnonics,” *Applied Physics Letters* **117**, 090501 (2020).
- [34] Anna-Luisa E. Römling, Alejandro Vivas-Viña, Carlos Sánchez Muñoz, and Akashdeep Kamra, “Resolving nonclassical magnon composition of a magnetic ground state via a qubit,” *Phys. Rev. Lett.* **131**, 143602 (2023).
- [35] Anna-Luisa E. Römling and Akashdeep Kamra, “Quantum sensing of antiferromagnetic magnon two-mode squeezed vacuum,” *Phys. Rev. B* **109**, 174410 (2024).
- [36] Eirik Erlandsen, Akashdeep Kamra, Arne Brataas, and Asle Sudbø, “Enhancement of superconductivity mediated by antiferromagnetic squeezed magnons,” *Physical Review B* **100**, 100503(R) (2019).
- [37] Eirik Erlandsen, Arne Brataas, and Asle Sudbø, “Magnon-mediated superconductivity on the surface of a topological insulator,” *Physical Review B* **101**, 094503 (2020).
- [38] Eirik Erlandsen and Asle Sudbø, “Schwinger boson study of superconductivity mediated by antiferromagnetic spin fluctuations,” *Physical Review B* **102**, 214502 (2020).
- [39] Even Thingstad, Eirik Erlandsen, and Asle Sudbø, “Eliashberg study of superconductivity induced by interfacial coupling to antiferromagnets,” *Physical Review B* **104**, 0114508 (2021).
- [40] Øyvind Johansen, Akashdeep Kamra, Camilo Ulloa, Arne Brataas, and Rembert A. Duine, “Magnon-Mediated Indirect Exciton Condensation through Antiferromagnetic Insulators,” *Physical Review Letters* **123**, 167203 (2019).
- [41] Jaechul Shim, Seok-Jong Kim, Se Kwon Kim, and Kyung-Jin Lee, “Enhanced Magnon-Photon Coupling at the Angular Momentum Compensation Point of Ferrimagnets,” *Physical Review Letters* **125**, 027205 (2020).
- [42] Jongjun M. Lee, Hyun-Woo Lee, and Myung-Joong Hwang, “Cavity magnonics with easy-axis ferromagnets: Critically enhanced magnon squeezing and light-matter interaction,” *Physical Review B* **108**, L241404 (2023).
- [43] Richard A. Beth, “Mechanical Detection and Measurement of the Angular Momentum of Light,” *Physical Review* **50**, 115–125 (1936).
- [44] Akashdeep Kamra, Utkarsh Agrawal, and Wolfgang Belzig, “Noninteger-spin magnonic excitations in textured magnets,” *Physical Review B* **96**, 020411 (2017).
- [45] Øyvind Johansen and Arne Brataas, “Nonlocal Coupling between Antiferromagnets and Ferromagnets in Cavities,” *Physical Review Letters* **121**, 087204 (2018).
- [46] Øyvind Johansen, *Antiferromagnetic Insulator Spintronics*, Ph.D. thesis, Norwegian University of Science and Technology (2019).
- [47] Assa Auerbach, *Interacting Electrons and Quantum Magnetism* (Springer, 1994).
- [48] Henning G. Hugdal, Stefan Rex, Flavio S. Nogueira, and Asle Sudbø, “Magnon-induced superconductivity in a topological insulator coupled to ferromagnetic and antiferromagnetic insulators,” *Physical Review B* **97**, 195438 (2018).
- [49] K. Kakazu and Y. S. Kim, “Quantization of electromagnetic fields in cavities and spontaneous emission,” *Physical Review A* **50**, 1830–1839 (1994).
- [50] Andreas T. G. Janssønn, Henning G. Hugdal, Arne Brataas, and Sol H. Jacobsen, “Cavity-mediated superconductor-ferromagnetic-insulator coupling,” *Physical Review B* **107**, 035147 (2023).
- [51] T. Holstein and H. Primakoff, “Field dependence of the intrinsic domain magnetization of a ferromagnet,” *Physical Review* **58**, 1098–1113 (1940).
- [52] A. V. Matetskiy, I. A. Kibirev, T. Hirahara, S. Hasegawa, A. V. Zotov, and A. A. Saranin, “Direct observation of a gap opening in topological interface states of MnSe/Bi₂Se₃ heterostructure,” *Applied Physics Letters* **107**, 091604 (2015).
- [53] N. Pournaghavi, M. F. Islam, Rajibul Islam, Carmine Autieri, Tomasz Dietl, and C. M. Canali, “Realization of the Chern-insulator and axion-insulator phases in antiferromagnetic MnTe/Bi₂(Se, Te)₃/MnTe heterostructures,” *Physical Review B* **103**, 195308 (2021).
- [54] Yusheng Hou, Jeongwoo Kim, and Ruqian Wu, “Magnetizing topological surface states of Bi₂Se₃ with a CrI₃ monolayer,” *Science Advances* **5**, eaaw1874 (2019).
- [55] Bevin Huang, Genevieve Clark, Efrén Navarro-Moratalla, Dahlia R. Klein, Ran Cheng, Kyle L. Seyler, Ding Zhong, Emma Schmidgall, Michael A. McGuire, David H. Cobden, Wang Yao, Di Xiao, Pablo Jarillo-Herrero, and Xiaodong Xu, “Layer-dependent ferromagnetism in a van der Waals crystal down to the monolayer limit,” *Nature* **546**, 270–273 (2017).
- [56] Nikhil Sivadas, Satoshi Okamoto, Xiaodong Xu, Craig J. Fennie, and Di Xiao, “Stacking-Dependent Magnetism in Bilayer CrI₃,” *Nano Letters* **18**, 7658–7664 (2018).
- [57] M. Soenen, C. Bacaksiz, R. M. Menezes, and M. V. Milosevic, “Stacking-dependent topological magnons in bilayer CrI₃,” *Physical Review Materials* **7**, 024421 (2023).
- [58] Haijun Zhang, Chao-Xing Liu, Xiao-Liang Qi, Xi Dai, Zhong

- Fang, and Shou-Cheng Zhang, “Topological insulators in Bi_2Se_3 , Bi_2Te_3 and Sb_2Te_3 with a single Dirac cone on the surface,” *Nature Physics* **5**, 438–442 (2009).
- [59] Dante J. O’Hara, Tiancong Zhu, Amanda H. Trout, Adam S. Ahmed, Yunqiu Kelly Luo, Choong Hee Lee, Mark R. Brenner, Siddharth Rajan, Jay A. Gupta, David W. McComb, and Roland K. Kawakami, “Room Temperature Intrinsic Ferromagnetism in Epitaxial Manganese Selenide Films in the Monolayer Limit,” *Nano Letters* **18**, 3125–3131 (2018).
- [60] Shahid Sattar, M. F. Islam, and C. M. Canali, “Monolayer MnX and Janus XMnY ($X, Y = \text{S}, \text{Se}, \text{Te}$): A family of two-dimensional antiferromagnetic semiconductors,” *Physical Review B* **106**, 085410 (2022).
- [61] Jiang Wang and Wen Wu, “Cavity-based linear-to-circular polarization converter,” *Optics Express* **25**, 3805–3810 (2017).
- [62] Hannes Hübener, Umberto De Giovannini, Christian Schäfer, Johan Andberger, Michael Ruggenthaler, Jerome Faist, and Angel Rubio, “Engineering quantum materials with chiral optical cavities,” *Nature Materials* **20**, 438–442 (2021).
- [63] Ruslan Salikhov, Igor Ilyakov, Lukas Körber, Attila Kákay, Rodolfo A. Gallardo, Alexey Ponomaryov, Jan-Christoph Deinert, Thales V. A. G. de Oliveira, Kilian Lenz, Jürgen Fassbender, Stefano Bonetti, Olav Hellwig, Jürgen Lindner, and Sergey Kovalev, “Coupling of terahertz light with nanometre-wavelength magnon modes via spin–orbit torque,” *Nature Physics* **19**, 529–535 (2023).
- [64] Andreas T. G. Janssønn, Haakon T. Simensen, Akashdeep Kamra, Arne Brataas, and Sol H. Jacobsen, “Macroscale nonlocal transfer of superconducting signatures to a ferromagnet in a cavity,” *Phys. Rev. B* **102**, 180506 (2020).
- [65] Jairo Sinova, Sergio O. Valenzuela, J. Wunderlich, C. H. Back, and T. Jungwirth, “Spin Hall effects,” *Reviews of Modern Physics* **87**, 1213–1260 (2015), 1411.3249.
- [66] Akashdeep Kamra and Lina G. Johnsen, “Nanoscale spin waves get excited,” *Nature Physics* **19**, 469–470 (2023).
- [67] Saima A. Siddiqui, Joseph Sklenar, Kisung Kang, Matthew J. Gilbert, André Schleife, Nadya Mason, and Axel Hoffmann, “Metallic antiferromagnets,” *Journal of Applied Physics* **128**, 040904 (2020).